Comparison of Sulfur Dioxide Removal Reactions Kinetics by Na_2CO_3 and Other Different Sorbents from Coal-fired Power Plants

I. Omidi Bibalani and H. Ale Ebrahim*
Department of Chemical Engineering,
Amirkabir University of Technology
(Tehran Polytechnic), Tehran, Iran

doi: https://doi.org/10.15255/CABEQ.2022.2069

Original scientific paper
Received: March 1, 2022
Accepted: October 26, 2022

This work deals with kinetic parameters estimation of Na_2CO_3+SO_2 reaction employing sophisticated random pore model. The temperature of experiments ranges from 100 to 250 °C, and various SO_2 concentrations are within 0.13–1.12 vol.%. According to the results, the reaction rate concentration dependency follows the fractional function. The values of rate constants and product layer diffusivities are expressed at various temperatures. Finally, it was attempted to describe the significance of this sorbent for SO_2 removal. Therefore, the kinetic results of Na_2CO_3+SO_2 reaction were compared with other similar studies on SO_2 reaction kinetics with CaO, CuO, and MgO sorbents. It was concluded that Na_2CO_3 shows advantages of higher rate constants, lower operating temperatures, and less possibility of incomplete conversion problem. The reported kinetic constants are essential for design of flue gas desulfurization reactors, especially in coal-fired power plants.

Keywords:
Na_2CO_3 sulfation, CaO sulfation, CuO sulfation, MgO sulfation, kinetics

Introduction

For preventing the acid rain problem, flue gas desulfurization (FGD) technologies include two main processes called throwaway and regeneration[1]. The throwaway process is suitable for relatively low SO_2 concentrations such as coal-fired power plants. On the other hand, regeneration methods are appropriate for high SO_2 concentrations, especially in copper smelters with further conversion of concentrated SO_2 to sulfuric acid or sulfur[1]. The sulfation reaction in coal-based power plants with SO_2 concentration of about 1000 ppm involves the throwaway method, where CaO (lime) is the most common sorbent. Because of the high ratio of molar volume of gypsum versus lime, pore mouth blockage and even incomplete conversion occur in the sulfation reaction of CaO_2. The comparison of kinetic parameters for SO_2 removal reactions by various sorbents is of great engineering importance and is the main goal of the present work.

Furthermore, to remove high SO_2 concentration from some non-ferrous metallurgical plants, dry and wet regeneration processes are appropriate. The elemental sulfur, as a valuable by-product, can be prepared through reduction of concentrated SO_2 stream with CH_4 as a reducing agent[3]. The principal sorbent of dry regenerative FGD process is CuO.

*Corresponding author: E-mail: alebrm@aut.ac.ir

The usual sorbents of dry FGD processes are different metal oxides and metal carbonates, including CaO, CuO, MgO, Fe_2O_3, Na_2CO_3, K_2CO_3, etc.[4–6]. The chemical reaction of Na_2CO_3 sorbent with SO_2 can be demonstrated as follows:

$$Na_2CO_3 + SO_2 + 0.5O_2 \rightarrow Na_2SO_4 + CO_2 \quad (1)$$

To survey the SO_2 adsorption efficiency by Na_2CO_3, many studies have been conducted. Electric Power Research Institute (EPRI) were the first to used dry sodium-based sorbent in 1977. The related experimental results revealed 70–90 % SO_2 removal for sub-bituminous coal combustion with various sodium-based sorbents containing a significant amount of Na_2CO_3[7]. Furthermore, multiple studies were carried out to investigate the influence of $NaHCO_3$ thermal decomposition on the Na_2CO_3 on SO_2 absorption yield[8–12]. The results demonstrated that the best performance could be achieved when the gas temperature ranges from 120 to 175 °C for the sulfation reaction of SO_2 with Na_2CO_3 sorbent. The enhancement effect of Na_2CO_3 addition on the promotion of limestone sulfate conversion, owing to enlarged surface area and tuned pore size distribution, was described by Han *et al.*[13] A packed scrubber with $NaHCO_3$ sorbent was employed by Ghorbani *et al.* to evaluate SO_2 concentration at the inlet and outlet of scrubber[14]. The results indicated the improvement of SO_2 removal efficiency through

cation surfactant additives[14]. In addition, Wu *et al.* used non-isothermal thermogravimetry to characterize the intrinsic kinetics of the thermal decomposition of $NaHCO_3$ to Na_2CO_3 via graphical and Friedman's procedures[15]. The first order reaction rate was determined by the amount of activation energy equaling 25.3 kcal mol^{-1}. They found that elevating the temperature of $NaHCO_3$ calcination from 120 to 230 °C would augment the pore diameter from 180 to 210 nm[15].

To remove SO_x and NO_x simultaneously, Mortson *et al.* applied a regenerated $NaHCO_3$/Na_2CO_3-based sorbent on an advanced FGD technology developed by AIRborne Technologies Inc. (ATI), producing various fertilizers with high SO_2 removal efficiency[16]. In order to absorb SO_2 and NO in a powder-particle fluidized bed reactor, Xu *et al.* used an Na_2CO_3/Al_2O_3 sorbent[17]. Different effective parameters such as temperature, mixtures composition, and sorbent size were tested[17]. Walawska *et al.* studied the structural factors of $NaHCO_3$ and Na_2CO_3 sorbents such as particle size, surface area, and pore volume[18]. They reported that Na_2CO_3 sorbent had better results in SO_2 removal yield and conversion rate[18]. Ma *et al.* presented a concept test of NOXSO flue gas treatment process at three scales of 0.017, 0.06, and 0.75 MW[19].

Concerning kinetic studies, Keener *et al.* applied shrinking core model neglecting solid reactant porosity to explain the sulfation reaction of $NaHCO_3$[20]. The model was applied to derive the equation of reaction rate constant as a function of temperature. The high dependency of reaction rate on temperature was reported by calculating the activation energy value (56.4 kJ mol^{-1})[20]. Kimura *et al.* studied the kinetics of Na_2CO_3 sulfation reaction at temperatures within 80–140 °C and 0.3 % SO_2 concentration via thermogravimetry[21]. Finally, rate constants were evaluated from the expressed mechanism and the experimental data[21]. In order to develop a model based on film theory consisting of diffusion, reaction, as well as thermodynamic equilibrium, Ebrahimi *et al.* used $NaHCO_3$/Na_2CO_3 sorbent for SO_2 elimination in a packed column[22]. Because of its simplicity, this model cannot predict a wide range of situations[22]. Charry Prada *et al.* carried out the sulfation reaction of $NaHCO_3$ in a fixed-bed reactor for 1500 ppm SO_2 and temperatures above 122 °C[23]. A solution method was applied to predict the reaction performance in this system with respect to length of the reactor. Thus, this study introduced an economic system in comparison with activated carbon sorbent to remove SO_2 for small-scale FGD applications[23].

As stated previously, lime-based FGD systems can be established only at high temperatures (about 800 °C). The value of molar volume of solid product to solid reactant for sulfation reaction of CaO is very high (Z=3). Hence, incomplete conversion phenomenon occurs owing to pore mouth blockage. On the other hand, the advantage of sulfation reaction by Na_2CO_3 sorbent is low operating temperature (about 200 °C). The lower Z value for Na_2CO_3 sulfation reaction (Z=1.28) is another superiority of this sorbent that offers the complete conversion possibility in the reaction with SO_2. Consequently, SO_2 elimination by Na_2CO_3 can be carried out at low temperatures with low sorbent consumption due to its complete conversions.

The sulfation reaction of solid sorbents such as Na_2CO_3, CaO, CuO, and MgO in FGD processes is one of the significant applications of non-catalytic gas-solid reactions. To examine the kinetics of these reactions, different mathematical models have been presented in the literature. Modified grain model and random pore model (RPM) are two comprehensive models for consideration of solid structural variations with time and specifically incomplete conversion. Because of considering the real porous sorbent pore size distribution by RPM, the higher accuracy of RPM for prediction of conversion-time profiles in comparison with the modified grain model was confirmed[24]. As mentioned, kinetic studies of sulfation reaction of Na_2CO_3 are very rare in literature. For example, Keener *et al.* employed sharp interface model for this reaction[20]. Because of neglecting Na_2CO_3 internal surfaces, the reported kinetic parameters were not real. On the other hand, Kimura *et al.* explored a porous model of Na_2CO_3 by assuming no diffusion resistance between sorbent nano-grains, but this assumption is unreliable[21]. Ultimately, inherent kinetic parameters of Na_2CO_3+SO_2 reaction are essential for the design of FGD reactors in coal-based power plants.

Recently, our group dealt with comprehensive kinetic study of Na_2CO_3 sulfation reaction by sophisticated RPM, evaluating concentration dependency, and applying the whole pore size distribution of the solid sorbent[25]. The resulting intrinsic kinetic parameters are required for reactor design of low temperature FGD systems. The current work presents a brief discussion of the conversion-time profiles of Na_2CO_3 sulfation reaction at various temperatures and different concentrations from isothermal thermogravimetry. In addition, comprehensive mathematical modeling of this reaction by applying RPM is explained. The concentration and temperature dependencies of the reaction rate and product layer diffusivities are expressed. The kinetics of SO_2 removal reactions by various sorbents including Na_2CO_3, CaO, CuO, and MgO are compared from the results of the literature kinetic studies. Thus, the main novelty of the present work is comparison of kinetic parameters of SO_2 removal reaction by different solid sorbents.

Materials and methods

The powder of $NaHCO_3$ (Chem-Lab) was pelletized at pressure of 60 bar in a 10-mm diameter die with a thickness of 1 mm. The pellet was placed in a thermogravimeter (TG) (Rheometric Scientific) for 30 minutes within a temperature range of 100–250 °C under zero air flow of 150 $cm^3\ min^{-1}$ to decompose and generate porous Na_2CO_3 for the reaction with SO_2. After calcination, a mixture of zero air and predefined concentration of SO_2 (0.13–1.12 vol.%) was applied under an isothermal condition to the TG, and the weight of sample pellet was plotted versus time. The experimental plot of conversion-time was obtained from the weight-time profile as:

$$X = \frac{m_t - m_i}{m_i}\left[\frac{M_{Na_2CO_3}}{M_{Na_2SO_4} - M_{Na_2CO_3}}\right] \tag{2}$$

To evaluate the pore size distribution of Na_2CO_3 pellet, nitrogen adsorption (by Autosorb-1MP from Quantachrome) and mercury porosimetry (by Carlo Erba) tests were performed on the calcined pellet. To determine the volume of micro- and meso-pores, Horvath-Kawazoe (HK) and Barrett-Joyner-Halenda (BJH) methods were employed. Meanwhile, the macro-pores distribution was obtained by Washburn equation. The results of the PSD within the range of 3–10000 A are presented in Fig. 1[25].

Modeling of reaction

The SO_2 removal reaction by Na_2CO_3 sorbent is a non-catalytic gas-solid reaction. To describe the accurate kinetics of such systems, the RPM initially recommended by Bhatia and Perlmutter was applied in this work. The RPM is the most precise and sophisticated non-catalytic gas-solid reaction model due to considering pore size distribution and solid structural changes during the reaction. The main dimensionless coupled partial differential equations of RPM for a slab pellet with general concentration dependency are expressed as[24,26]:

$$\frac{\partial}{\partial y}\left(\delta\frac{\partial a}{\partial y}\right) = \frac{\phi^2 f(a) b\sqrt{1-\psi\ln b}}{1+\frac{\beta Z}{\psi}\left[\sqrt{1-\psi\ln b}-1\right]} \tag{3}$$

$$\frac{\partial b}{\partial \theta} = -\frac{f(a) b\sqrt{1-\psi\ln b}}{1+\frac{\beta Z}{\psi}\left[\sqrt{1-\psi\ln b}-1\right]} \tag{4}$$

Equation (3) is pseudo-steady state diffusion-reaction conservation equation for gaseous reactant, while Equation (4) is unsteady conservation equation for the solid reactant. In the above equations, a and b denote dimensionless gaseous and solid reactants concentrations, ψ represents pore structural parameter of the RPM, φ is the Thiele modulus, and β shows product layer resistance. Z is a significant parameter in the RPM, which is defined as the ratio of the molar volume of the solid

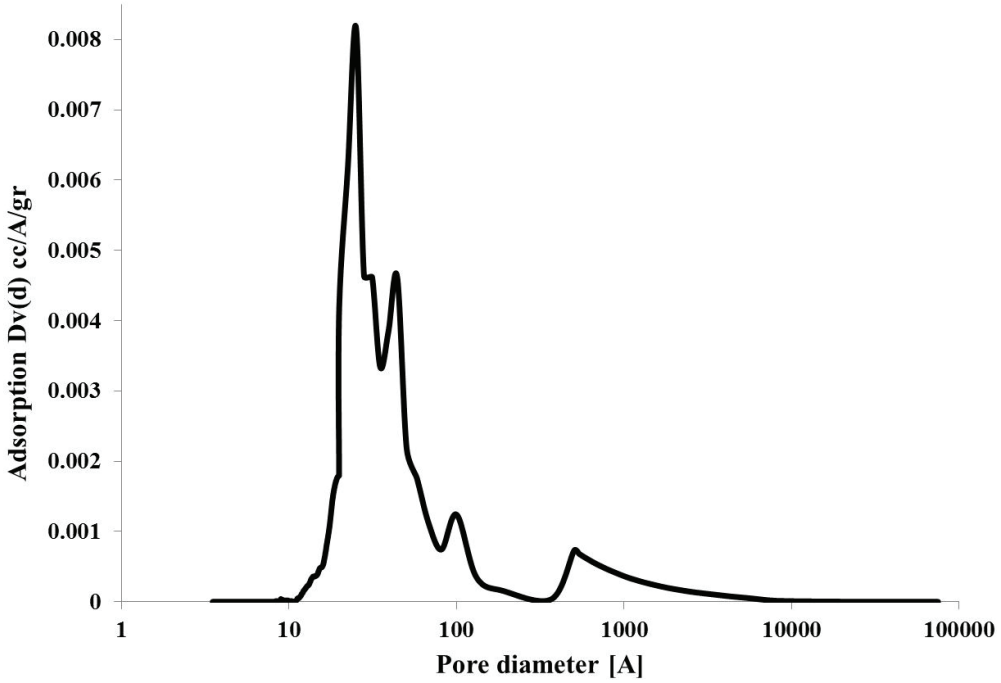

Fig. 1 – *PSD of Na_2CO_3 pellet*[25]

product to the solid reactant. When $Z>1$, the porosity diminishes during the reaction due to volume expansion. Because of the blockage of pore mouths at high Z values, incomplete conversion can occur. The Z values for sulfation reactions of MgO, CuO, CaO, and Na_2CO_3 are 4.0, 3.52, 3.0, and 1.28, respectively. Thus, the lower Z value for Na_2CO_3 reaction with SO_2 is a positive point for the relevant FGD reaction.

The effective axial diffusivity of SO_2 along the pores of pellet is calculated from molecular diffusion (D_{AM}) and the Knudsen diffusivity (D_{AK}) by the following equations[24,27,29]:

$$\delta = \frac{D_e}{D_{e0}} = (\frac{\varepsilon}{\varepsilon_0})^2 = [1 - \frac{(Z-1)(1-\varepsilon_0)(1-b)}{\varepsilon_0}]^2 \quad (5)$$

$$\frac{1}{D_{e_0}} = \frac{1}{\varepsilon_0^2}(\frac{1}{D_{AM}} + \frac{1}{D_{AK}}) \quad (6)$$

$$D_{AM} = \frac{1.859 \cdot 10^{-3} T^{1.5} \sqrt{\frac{1}{M_1} + \frac{1}{M_2}}}{p\sigma_{12}^2 \Omega} \quad (7)$$

$$D_{AK} = \frac{2r_{av}}{3}\sqrt{\frac{8R_g T}{\pi M_A}} \quad (8)$$

To calculate the main RPM parameter (ψ), the following formulas are used:

$$V_p = \int_0^\infty \nu_0(r)\mathrm{d}r \quad (9)$$

$$\varepsilon_0 = \frac{V_p}{V_p + \frac{1}{\rho_B}} \quad (10)$$

$$r_{av} = \frac{1}{V_p + \frac{1}{\rho_B}} \int_0^\infty \nu_0(r) r \mathrm{d}r \quad (11)$$

$$S_0 = \frac{2}{V_p + \frac{1}{\rho_B}} \int_0^\infty \frac{\nu_0(r)}{r}\mathrm{d}r \quad (12)$$

$$L_0 = \frac{1}{\pi(V_p + \frac{1}{\rho_B})} \int_0^\infty \frac{\nu_0(r)}{r^2}\mathrm{d}r \quad (13)$$

$$\psi = \frac{4\pi L_0 (1-\varepsilon_0)}{S_0^2} \quad (14)$$

Results

Order of the reaction

To estimate the best order of the reaction, the previous equations were solved by shooting method, which replaced δ and b as unity at the zero times of reaction when the product layer thickness around the pores was negligible. The following formula was established by differentiation of simplified equations for initial slope of conversion-time profile of the sulfation reaction:

$$[\frac{\mathrm{d}X}{\mathrm{d}\theta}]_{\theta\to 0} = \int_0^1 F(y)\mathrm{d}y \quad (15)$$

Equation (15) can be reformulated by inserting the relation between actual time and θ as[24,27,30]:

$$I = \frac{C_{B0}(1-\varepsilon_0)}{S_0 \int_0^1 F(y)\mathrm{d}y}[\frac{\mathrm{d}X}{\mathrm{d}t}]_{t\to 0} = k_s C_{Ab}^n \quad (16)$$

The highest correlation coefficient of I versus $_{Ab}$ plot, specifies the best order of reaction. Hence, to survey the concentration dependency, a series of experiments was conducted at 150 °C and within 0.13–1.12 vol.% SO_2 concentration, with the results of correlation coefficients reported in Table 1[25].

Thus, the fractional form was suggested from Table 1 to qualify as the best concentration dependency of Na_2CO_3 reaction with SO_2 due to higher regression coefficient.

Table 1 – *Regression coefficients of different concentration functions of Na_2CO_3 sulfation*[25]

$f(a)$	$a^{0.89}$	$a^{0.9}$	$a^{0.92}$	$a^{0.98}$	$a^{1.0}$	$a^{1.15}$	$\frac{C_{Ab}\, a}{1 + K_{ad} C_{Ab}\, a}$
R^2	0.955	0.951	0.951	0.937	0.933	0.922	0.970

Table 2 – *Rate constants of Na_2CO_3 sulfation at various temperatures*[25]

T (°C)	100	125	150	175	200	225	250
$k_s \cdot 10^6$ (m s^{-1})	8.78	26.8	34.8	53.5	60.9	66.5	91.4

Rate constants

To attain the k_s values at different temperatures, iteration method was established using Equation (16). An Arrhenius plot was employed to estimate the frequency factor and activation energy. For this purpose, various experiments were carried out at 0.66 vol.% SO_2 concentration and temperatures within 100–250 °C plus conversion-time curves, as presented in Fig. 2[25]. The values of k_s at different temperatures are summarized in Table 2[25].

Fig. 3 illustrates the Arrhenius plot of these data, where the rate constant's temperature dependency is expressed as follows[25]:

$$k_s = 1.8 \cdot 10^{-2} \exp(\frac{-22486.04}{RT}) \quad (17)$$

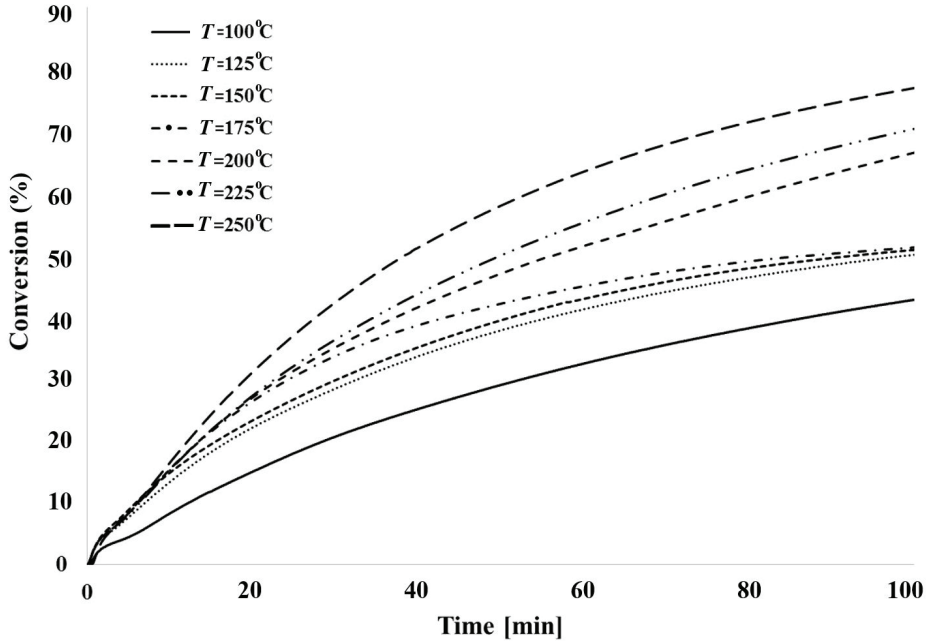

Fig. 2 – *Experimental conversion-time profiles of sulfation reaction of Na_2CO_3 at 0.66 vol.% SO_2*[25]

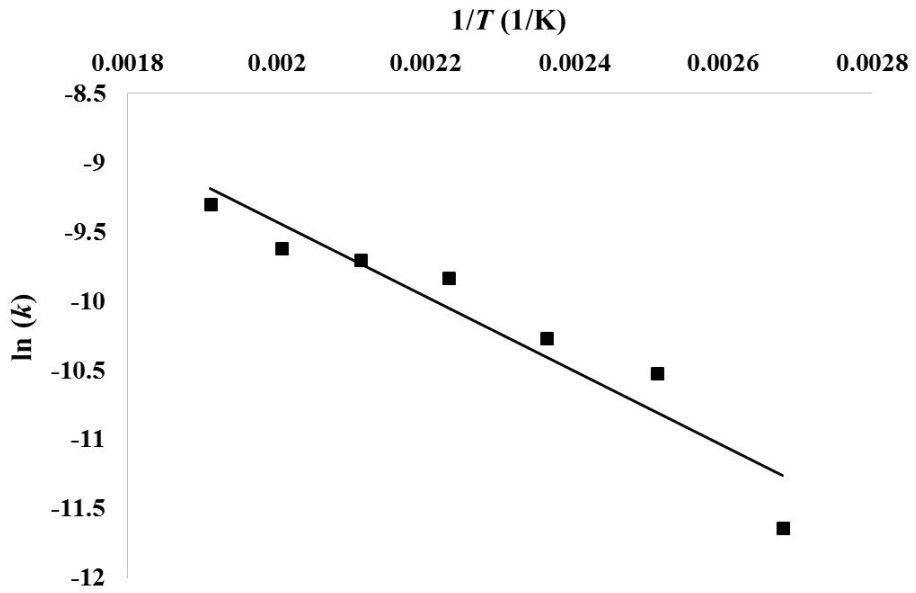

Fig. 3 – *Arrhenius plot of Na_2CO_3 sulfation reaction rate constants*[25]

Product layer diffusion

According to the RPM principle, SO_2 radial product layer diffusivity around each pore (D_p) can be evaluated as a fitting parameter through comparison between the conversion-time profiles obtained from solving the governing coupled partial differential RPM equations numerically (by Matlab software) and experimental data. Thus, a D_p value was guessed and the coupled partial differential equations were solved by finite element method. The best fit with all experimental conversion-time points generated appropriate values for SO_2 diffusivity in the product layer (Na_2SO_4). The obtained D_p values at different temperatures are presented in Table 3[25]. The RPM conversion-time predictions and experimental profiles at various temperatures are plotted

Table 3 – *SO_2 diffusivity through product layer of Na_2CO_3 sulfation at various temperatures*[25]

T (°C)	100	125	150	175	200	225	250
$D_p \cdot 10^{18}$ (m^2 s^{-1})	1.25	3.00	3.40	3.95	6.60	8.00	15.00

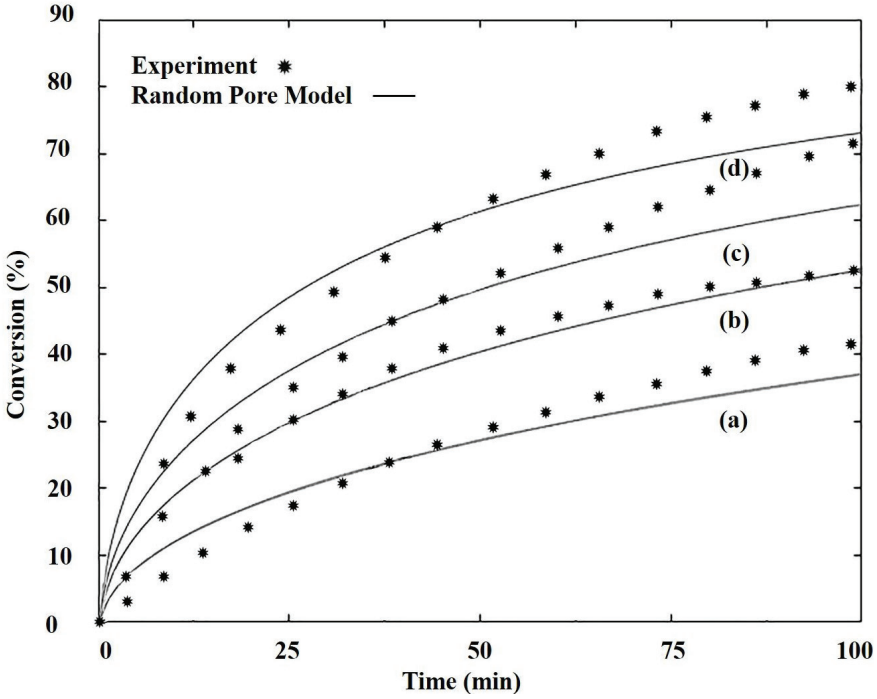

Fig. 4 – *Comparison of RPM predictions with experimental data for Na_2CO_3 reaction with 0.66 vol.% SO_2, a)100 °C, b) 150 °C, c) 200 °C, d) 250 °C* [25]

in Fig. 4[25]. As this figure indicates, the agreement of RPM predictions and experimental data is reasonably good.

Table 4 presents the main structural parameters of Na_2CO_3 pellet[25].

Finally, D_p as a function of temperature can be stated with the following formula [25]:

$$D_P = 3 \cdot 10^{-15} \exp\left(\frac{-23354.03}{RT}\right) \qquad (18)$$

Discussion

The main application of sulfation reactions of Na_2CO_3, CaO, CuO and MgO is SO_2 elimination. In this part, based on the obtained results of this study and other similar investigations in the literature, rate constants, Z values, and diffusivities of the aforementioned sorbents are compared.

Table 4 – *Structural parameters of RPM for Na_2CO_3 pellet after calcination*[25]

Pellet	$\bar{r}$ [cm]	ε_0	L_0 [cm^{-2}]	S_0 [cm^{-1}]	ψ
Na_2CO_3	$1.92 \cdot 10^{-5}$	0.64	$1.36 \cdot 10^{12}$	$1.27 \cdot 10^{6}$	3.81

Table 5 reports the rate constant equations and diffusion coefficients of SO_2 through the product layers for different sorbents extracted from previous works and this study.

The values of these mentioned parameters and *Z* values were calculated within the range of reported operating temperatures, with the results summarized in Table 6. It is obvious from Table 6 that the rate constant of Na_2CO_3 is higher than that of other similar sorbents.

To compare the rate constant of this study with other works, the approximate solution of RPM governing equations was rearranged as[31]:

$$\frac{dX}{dt} = \frac{\dfrac{k_s S_0 C_{Ab}}{\rho_B (1-\varepsilon_0)}}{\dfrac{\dfrac{\beta Z}{\psi}}{\dfrac{1}{1-X}}\left[\left(\dfrac{\beta Z}{\psi}\left(\dfrac{1}{\psi} - \ln(1-X)\right)\right)^{0.5} + \dfrac{1}{\beta Z^{0.5}} - \dfrac{\beta Z^{0.5}}{\psi}\right]}{\left(\dfrac{\beta Z}{\psi}\left(\dfrac{1}{\psi} - \ln(1-X)\right)\right)^{0.5}} + \dfrac{\phi^2}{6}\dfrac{\dfrac{2}{(1-X)^{1/3}} - 2}{\left(1 - \dfrac{(Z-1)(1-\varepsilon_0 X)}{\varepsilon_0}\right)^2}} \qquad (19)$$

Table 5 – *Rate constants of previous studies on different sorbents*

	Sorbent	T (°C)	Order of reaction	Kinetic model	Rate constant	unit	ref
1	Na_2CO_3	100–250	Fractional	Random pore model	$k = 1.8 \cdot 10^{-2} \exp\left(\frac{-22486}{RT}\right)$ $D_p = 3.0 \cdot 10^{-15} \exp\left(\frac{-23354}{RT}\right)$	m s^{-1}	25
2	CaO	850–925	First order	Random pore model	$k = 0.1272 \exp\left(\frac{-93920}{RT}\right)$ $D_p = 3.24 \cdot 10^{-11} \exp\left(\frac{-1758}{RT}\right)$	m s^{-1} m^2 s^{-1}	29
3	CuO	400–600	First order	Random pore model	$k = 8.169 \cdot 10^{-3} \exp\left(\frac{-78807}{RT}\right)$ $D_p = 2.287 \cdot 10^{-11} \exp\left(\frac{-106519}{RT}\right)$	m s^{-1} m^2 s^{-1}	27
4	CuO	400–600	First order	Modified grain model	$k = 2.724 \cdot 10^{-1} \exp\left(\frac{-95503}{RT}\right)$ $D_p = 1.779 \cdot 10^{-10} \exp\left(\frac{-112231}{RT}\right)$	m s^{-1} m^2 s^{-1}	24
5	CuO	400–600	First order	Volume reaction model	$k = 2.22 \cdot 10^{2} \exp\left(\frac{-81777}{RT}\right)$	m^3 kmol^{-1} s^{-1}	24
6	MgO	500–700	Fractional	Random pore model	$k = 2.38 \cdot 10^{-3} \exp\left(\frac{-38629}{RT}\right)$ $D_p = 3.28 \cdot 10^{-14} \exp\left(\frac{-68474}{RT}\right)$	m s^{-1} m^2 s^{-1}	30
7	$NaHCO_3$	120–175	First order	Shrinking core model	$k = 2.262 \cdot 10^{6} \exp\left(\frac{-13.512}{RT}\right)$	cm s^{-1}	20

Table 6 – *Surface rate constants, Z values, and SO_2 diffusivities of various sorbents*

Sorbent	Temperature range (°C)	S_0 (m^2 m^{-3})	$k_S \cdot 10^8$ (m s^{-1})	$D_p \cdot 10^{19}$ (m^2 s^{-1})	Z	$k_s \cdot S_0$ (s^{-1})	Ref.
Na_2CO_3	100–250	$1.27 \cdot 10^8$	878 – 9139	12–150	1.28	1115–11606	25
CaO	850–925	$1.15 \cdot 10^8$	544 – 1023	2.3–7.8	3.0	600–1100	29
CuO	400–600	$5.4 \cdot 10^8$	0.6 – 16	1.2–96	3.52	3.2–87	27
MgO	500–700	$6.32 \cdot 10^8$	584 – 1998	7.8–69	4.0	3691–12627	30

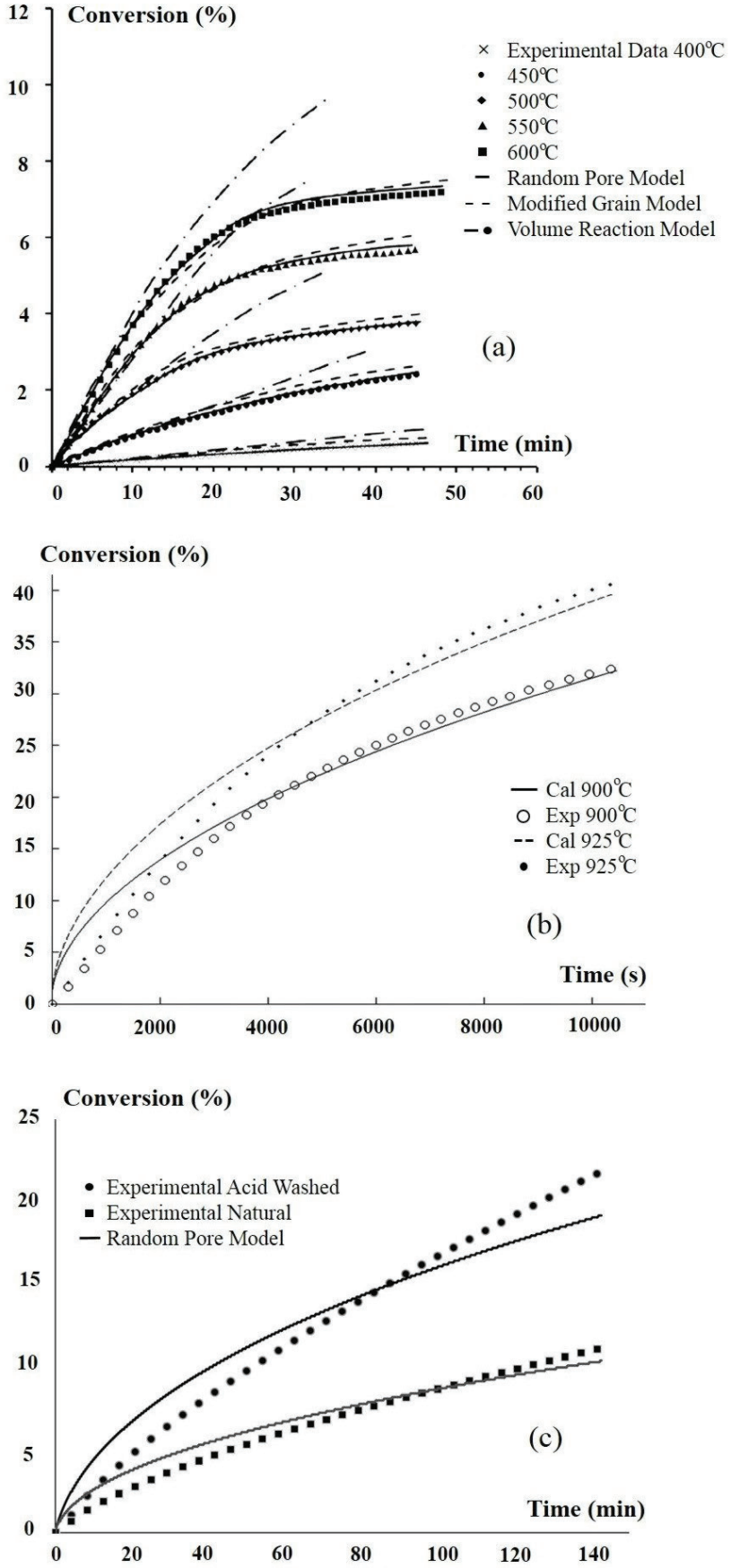

Fig. 5 – *Conversion-time profiles for sulfation reaction of: a) CuO[24], b) CaO[29], c) MgO[30]*

Hence, k_sS_0 is the efficient kinetic term in conversion-time improvement, which is listed in the right column of Table 6. It is clear from Table 6 that values of k_sS_0 for CuO sorbent are low, while those for the CaO sorbent are within the medium range. Meanwhile, k_sS_0 values for Na_2CO_3 and MgO sorbents are relatively high. Finally, it was concluded that high values of k_sS_0 for Na_2CO_3 and MgO sorbents could reduce the required residence time in an industrial FGD reactor for these sorbents. The size of these reactors can be reduced for more efficient sorbents (Na_2CO_3 and MgO), and thus the capital cost lowered.

The values of SO_2 diffusivities through the product layer generated from sulfation reactions of CuO and CaO sorbents are low. The diffusion coefficients in the product layer for MgO and Na_2CO_3 sorbents are in the medium range.

As stated previously, the value of Z is an important parameter for progression of the reaction due to possibility of the pore mouths blockage. For the reaction of sodium carbonate sorbent with SO_2, the value of Z is 1.28, which is minimum in Table 6. Conversion-time profiles of SO_2 removal reactions by CaO, CuO, and MgO sorbents are illustrated in Fig. 5. It is obvious from comparison of Fig. 4 and Fig. 5 that the lower value of Z for Na_2CO_3 sulfation reaction is a superior condition to achieve higher conversions in comparison with the other aforementioned sorbents.

The last major advantage of Na_2CO_3 sorbent for SO_2 removal reaction is its ability to operate at lower temperatures (second column of Table 6).

Conclusion

In this study, the inherent kinetic parameters of Na_2CO_3 reaction with SO_2 were presented using sophisticated RPM. The fractional concentration dependency was specified for the reaction rate and its activation energy was obtained as 22.5 kJ mol^{-1}.

The diffusion coefficient of SO_2 through the product layer was established as a function of temperature with values ranging from $12.5\cdot10^{-19}$ m^2 s^{-1} to $15\cdot10^{-18}$ m^2 s^{-1} when temperature changed from 100 to 250 °C. The results of Na_2CO_3 sulfation reaction in comparison with CaO, CuO, and MgO sorbents revealed a higher rate constant. Thus, Na_2CO_3 sulfation reaction progresses significantly at initial times. The incomplete conversion possibility for Na_2CO_3 was lower than for other sorbents due to its lower Z value. Finally, Na_2CO_3 potential to react with SO_2 within a low temperature range is the main superiority of this sorbent versus similar CaO, CuO, and MgO sorbents.

CONFLICT OF INTEREST

Authors state that there is no conflict of interest.

Nomenclature

$a = C_A/C_{Ab}$ – Dimensionless gas concentration
$b = C_B/C_{B0}$ – Dimensionless solid concentration
C_A – Gaseous reactant concentration in pellet, kmol m^{-3}
C_{Ab} – Bulk gas concentration, kmol m^{-3}
C_B – Solid reactant concentration, kmol m^{-3}
C_{B0} – Initial solid reactant concentration, kmol m^{-3}
D_{AK} – Knudsen diffusivity, m^2 s^{-1}
D_{AM} – Molecular diffusivity of gas A in pellet, m^2 s^{-1}
D_e – Effective diffusivity of gas A in pellet, m^2 s^{-1}
D_{e0} – Initial effective diffusivity of gas A in pellet, m^2 s^{-1}
D_p – Effective diffusivity of gas A in product layer, m^2 s^{-1}
k_m – External mass transfer coefficient, m s^{-1}
k_s – Surface rate constant, m s^{-1}
K_{ad} – Adsorption constant, m^3 kmol^{-1}
L – Thickness of pellet, m
L_0 – Pore length per unit volume, m^{-2}
M_B – Molecular weight of solid reactant, kg kmol^{-1}
M_D – Molecular weight of solid product, kg kmol^{-1}
n – Reaction order
r – Pore radius, m
$\bar{r}$ – Average pore radius of pellet, m
R – Gas constant, J K^{-1} mol^{-1}
S_0 – Reaction surface area per unit volume, m^{-1}
$Sh = k_mL/2D_{AM}$ – Sherwood number for external mass transfer
t – Time, s
$v_0(r)$ – Pore volume distribution function, m^2 kg^{-1}
V_p – Total pore volume, m^3 kg^{-1}
$X(\theta)$ – Solid conversion at each time
$y = 2z/L$ – Dimensionless position in pellet
z – Distance from center of pellet, m
Z – Ratio of molar volume of solid product to solid reactant
$\beta = 2k_s(1-\varepsilon_0)/(v_BD_pS_0)$ – Product layer resistance
ε – Pellet porosity

ε_0 – Initial pellet porosity

$\delta=D_e/D_{e0}$ – Variation ratio of pore diffusion

$\theta=k_s S_0 C_{Ab}^{\ n} t/[C_{B0}(1-\varepsilon_0)]=t/\tau$ – Dimensionless time

ν_B – Stoichiometric coefficient of solid reactant

ν_D – Stoichiometric coefficient of solid product

ρ_B – True density of solid reactant, kg m^{-3}

ρ_D – True density of solid product, kg m^{-3}

$\theta=(L/2)(k_s S_0 C_{Ab}^{\ n-1}/\nu_B D_{e0})^{1/2}$ – Thiele modulus for pellet

ψ – Main RPM parameter

References

1. *Kirk, R. E., Othmer, D. F., Mann, C. A.*, Encyclopedia of Chemical Technology, (1994), Vol. II.
2. *Ale Ebrahim, H.*, Application of random-pore model to SO_2 capture by lime, Ind. Eng. Chem. Res. **49** (2010) 117. doi: https://doi.org/10.1021/ie901077b
3. *Mousavi, S. E., Pahlavanzadeh, H., Khani, M., Ale Ebrahim, H., Mozaffari, A.*, Selective catalytic reduction of SO_2 with methane for recovery of elemental sulfur over nickel-alumina catalysts, React. Kinet. Mechanis. Catal. **124** (2018) 669. doi: https://doi.org/10.1007/s11144-018-1360-x
4. *Gray, S. M., Jarvis, J. B.*, Process for removing SO_2 from flue gases using liquid sorbent injection, Google Patents, 2020.
5. *Tseng, H.-H., Wey, M.-Y.*, Study of SO_2 adsorption and thermal regeneration over activated carbon-supported copper oxide catalysts, Carbon **42** (2004) 2269. doi: https://doi.org/10.1016/j.carbon.2004.05.004
6. *Jia, Z., Liu, Z., Zhao, Y.*, Kinetics of SO_2 removal from flue gas on CuO/Al_2O_3 sorbent catalyst, Chem. Eng. Tech. **30** (2007) 1221. doi: https://doi.org/10.1002/ceat.200700139
7. *Bland, V.*, Evaluation of dry sodium sorbent utilization in combustion gas SOx/NOx reduction; Electric Power Research Institute, 1990.
8. *Carson, J. R.*, Removal of sulfur dioxide and nitric oxide from a flue gas stream by two sodium alkalis of various sizes, 1980.
9. *Dal Pozzo, A., Moricone, R., Tugnoli, A., Cozzani, V.,* Experimental investigation of the reactivity of sodium bicarbonate toward hydrogen chloride and sulfur dioxide at low temperatures, Ind. Eng. Chem. Res. **58** (2019) 6316. doi: https://doi.org/10.1021/acs.iecr.9b00610
10. *Erdos, E., Mocek, K., Lippert, E., Uchytilova, V., Neuzil, L.*, Application of the active soda process for removing sulphur dioxide from flue gases, JAPCA **39** (1989) 9. doi: https://doi.org/10.1080/08940630.1989.10466613
11. *Knight, J. H.*, The use of nahcolite for removal of sulfur dioxide and nitrogen oxides from flue gas. The Superior Oil Company, 1977.
12. *Mocek, K., Beruto, D.*, On the morphological nature of Na_2CO_3 produced by thermal decomposition from $NaHCO_3$ and from $Na_2CO_3 \cdot 10H_2O$, Mat. Chem. Phys. **14** (1986) 219. doi: https://doi.org/10.1016/0254-0584(86)90035-0
13. *Han, R., Sun, F., Gao, J., Wei, S., Su, Y., Qin, Y.*, Trace Na_2CO_3 addition to limestone inducing high-capacity SO_2 capture, Environ. Sci. Technol. **51** (2017) 12692. doi: https://doi.org/10.1021/acs.est.7b04141
14. *Ghorbani Shahna, F., Bahrami, A., Rotivand, F., Salari, S.*, Evaluation the effects of using surfactants with sodium bicarbonate and limestone for the removal of sulfur dioxide in packed scrubber, Ir. Occupat. Heal J. **14** (2017) 162.
15. *Wu, Y.-L., Shih, S.-M.*, Intrinsic kinetics of the thermal decomposition of sodium bicarbonate, Thermochim. Acta **223** (1993) 177. doi: https://doi.org/10.1016/0040-6031(93)80132-T
16. *Mortson, M., Telesz, R. W.*, Flue gas desulfurization using recycled sodium bicarbonate. In The US EPA/DOE/EPRI Combined Power Plant Air Pollutant Control, The Mega Symposium, 2001.
17. *Xu, G., Luo, G., Akamatsu, H., Kato, K.*, An adaptive sorbent for the combined desulfurization/denitration process using a powder-particle fluidized bed, Ind. Eng. Chem. Res. **39** (2000) 2190. doi: https://doi.org/10.1021/ie9908027
18. *Walawska, B., Szymanek, A., Pajdak, A., Nowak, M.*, Flue gas desulfurization by mechanically and thermally activated sodium bicarbonate, Pol. J. Chem. Technol. **16** (2014) 56. doi: https://doi.org/10.2478/pjct-2014-0051
19. *Ma, W., Haslbeck, J.*, NOxSO SO_2/NOx flue gas treatment process Proof-of-Concept test, Environ. Prog. **12** (1993) 163. doi: https://doi.org/10.1002/ep.670120303
20. *Keener, T. C., Khang, S.-J.*, Kinetics of the sodium bicarbonate—sulfur dioxide reaction, Chem. Eng. Sci. **48** (1993) 2859. doi: https://doi.org/10.1016/0009-2509(93)80032-L
21. *Kimura, S., Smith, J.*, Kinetics of the sodium carbonate–sulfur dioxide reaction, AIChE J. **33** (1987) 1522. doi: https://doi.org/10.1016/0009-2509(93)80032-L
22. *Ebrahimi, S., Picioreanu, C., Kleerebezem, R., Heijnen, J., Van Loosdrecht, M.*, Rate-based modelling of SO_2 absorption into aqueous $NaHCO_3/Na_2CO_3$ solutions accompanied by the desorption of CO_2, Chem. Eng. Sci. **58** (2003) 3589. doi: https://doi.org/10.1016/S0009-2509(03)00231-8
23. *Charry Prada, I. D., Rivera-Tinoco, R., Bouallou, C.*, Flue gas desulfurization assessment by modeling and experimental work of an optimized fixed-bed $NaHCO_3$ reactor, Ind. Eng. Chem. Res. **58** (2019) 18717. doi: https://doi.org/10.1021/acs.iecr.9b03010
24. *Bahrami, R., Ale Ebrahim, H., Halladj, R.*, Comparison of random pore model, modified grain model, and volume reaction model predictions with experimental results of SO_2 removal reaction by CuO, J. Ind. Eng. Chem. **30** (2015) 372. doi: https://doi.org/10.1016/j.jiec.2015.06.006
25. *Omidi Bibalani, I., Ale Ebrahim, H.*, Kinetic study of low temperature sulfur dioxide removal reaction by sodium carbonate using random pore model, Environ. Sci. Pollut. Res. **29** (2022) 6334. doi: https://doi.org/10.1007/s11356-021-16073-w
26. *Bahrami, R., Ale Ebrahim, H., Halladj, R., Afshar, A.*, A comprehensive kinetic study of the SO_2 removal reaction by pure CuO with the random pore model, Prog. React. Kinet. Mechanis **41** (2016) 385. doi: https://doi.org/10.3184%2F146867816X14716171449503
27. *Bahrami, R., Ale Ebrahim, H., Halladj, R.*, Application of random pore model for SO_2 removal reaction by CuO, Proc. Saft. Environ. Protect. **92** (2014) 938. doi: https://doi.org/10.1016/j.psep.2013.11.002
28. *Bhatia, S., Perlmutter, D.*, A random pore model for fluid-solid reactions: II. Diffusion and transport effects, AIChE J. **27** (1981) 247. doi: https://doi.org/10.1002/aic.690270211

29. *Moshiri, H., Nasernejad, B., Ale Ebrahim, H., Taheri, M.*, A comprehensive kinetic study of the reaction of SO_2 with CaO by the random pore model, Chem. Eng. Technol. **37** (2014) 2037.
doi: https://doi.org/10.1002/ceat.201400285
30. *Bakhshi Ani, A., Ale Ebrahim, H.*, Theoretical and experimental investigation on improvement of magnesium oxide sorbent by acetic acid washing for enhancing flue gas desulfurization performance, Chem. Pap. **74** (2020) 2471.
doi: https://doi.org/10.1007/s11696-020-01093-6
31. *Sohn, H., Chaubal, P.*, Approximate closed-form solutions to various model equations for fluid-solid reactions, AIChE J. **32** (1986) 1574.
doi: https://doi.org/10.1016/j.enconman.2013.04.044